

## Authors' responses to Referees' comments

**Journal:** Atmospheric Chemistry and Physics (ACP)

**Manuscript Number:** ACP-2025-898

**Title:** Vertically Resolved Formation Mechanisms of Fine Particulate Nitrate in Asian Megacities: Synergistic Lidar-Aircraft Observations and Process-Based Analysis

**Authors:** Yutong Tian, Ting Yang, et al.

Note:

Comment (13-point black italicized font).

Reply (indented, 13-point blue normal font).

“Revised text as it appears in the text (in quotes, 12-point blue italicized font)”.

---

## Anonymous Referee #2

### 1 General comments:

*The manuscript addresses an important environmental issue, vertical formation mechanism of nitrates in Asian megacities. It is overall well written, providing important progress through vertically continuous observations and comprehensive data analysis. My specific comments are as follows.*

### Authors' response:

We thank the reviewer for the positive assessment and constructive suggestions of our manuscript.

### 2 Detailed Comments:

*1) It's recommended to change the title from "Synergistic Lidar - Aircraft Observations and Process - Based Analysis" to "Integrated Lidar - Aircraft Observations and Process Analysis".*

### Authors' response:

Thanks for your suggestion. Accordingly, we have revised the title from “Synergistic Lidar – Aircraft Observations and Process-Based Analysis” to “Integrated Lidar – Aircraft Observations and Process Analysis” to improve clarity and conciseness.

*2) In the Data and Methods section, include more details about the machine learning*

*model (such as algorithm name, input variables, R2 value for validation accuracy) and cite relevant studies.*

**Authors' response:**

Thanks for your suggestion. In the revised manuscript we have substantially expanded the Data and Methods section to specify that we use a hybrid convolutional neural network (CNN)–long short-term memory (LSTM) mapping model (Hinton et al., 2006; Wang et al., 2016) whose hyperparameters are automatically tuned via Bayesian optimization (Frazier, 2018). We now clearly list all twelve input variables—six optical retrievals (AN, AW, WSOM, WIOM, BC, extinction at 532 nm) plus geopotential height, relative humidity, temperature, and the u, v, w wind components—and state that the model outputs mass concentrations of  $\text{NH}_4^+$ ,  $\text{NO}_3^-$ ,  $\text{SO}_4^{2-}$ , OM and BC with hourly resolution and 60 vertical layers (0.15–6.00 km).

Validation against independent ground-truth measurements from an Aerodyne Aerosol Chemical Speciation Monitor (ACSM) yields  $R^2$  values for  $\text{NH}_4^+$ ,  $\text{NO}_3^-$ ,  $\text{SO}_4^{2-}$ , OM and BC of 0.70, 0.69, 0.62, 0.61, and 0.58, respectively, with root-mean-square errors of 0.96–7.67  $\mu\text{g m}^{-3}$  and normalized mean biases within 0.012 (Figure R1). These results are provided in the Supplementary Information. Moreover, in our previous publications, we have validated these vertical profiles against aircraft measurements (Song et al., 2025; Tan et al., 2025), achieving correlation coefficients above 0.94 and root mean square errors below 7.9, and demonstrating a strong agreement between the retrieved profiles and airborne observations as Figure R2.

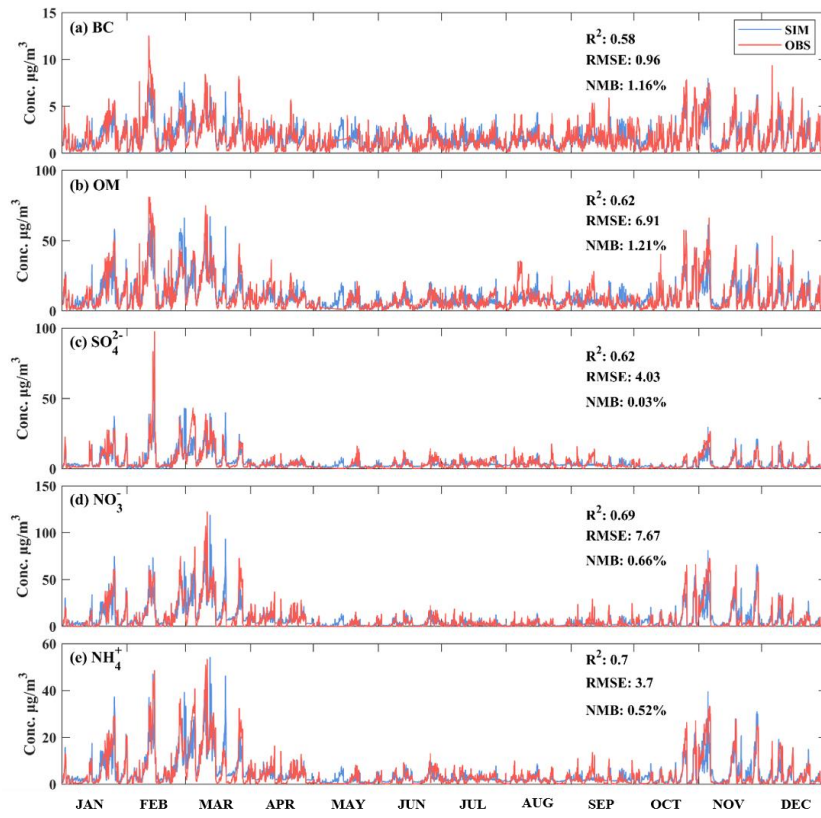


**Figure R1. Validation of ground-layer retrieval results against ACSM observations.**

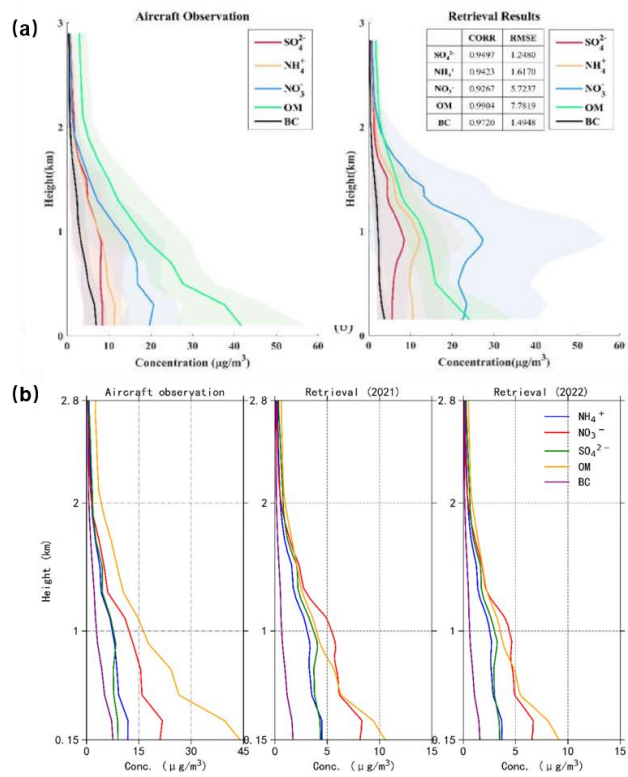


**Figure R2. Vertical profile validation against 2016 aircraft measurements: 2022 Winter Olympics (a); 2021–2022 (b).**

## Reference

- Frazier, P.: A Tutorial on Bayesian Optimization, ArXiv, abs/1807.02811, 2018.
- Hinton, G. E., Osindero, S., and Teh, Y.-W.: A Fast Learning Algorithm for Deep Belief Nets, *Neural Computation*, 18, 1527-1554, 10.1162/neco.2006.18.7.1527, 2006.
- Song, Y., Yang, T., Tian, P., Li, H., Tian, Y., Tan, Y., Sun, Y., and Wang, Z.: Novel Insights into the Vertical Distribution Patterns of Multiple PM<sub>2.5</sub> Components in a Super Mega-City: Responses to Pollution Control Strategies, 10.3390/rs17071151, 2025.
- Tan, Y., Yang, T., Li, H., Tian, P., Song, Y., He, J., Tian, Y., Sun, Y., and Wang, Z.: Unveiling the vertical dynamics of atmospheric ammonium in Asia megacity: A GRASP-based investigation of spatiotemporal patterns and source drivers, *Atmospheric Research*, 325, 108201, <https://doi.org/10.1016/j.atmosres.2025.108201>, 2025.
- Wang, M., Song, L., Yang, X., and Luo, C.: A parallel-fusion RNN-LSTM architecture for image caption generation, 2016 IEEE International Conference on Image Processing (ICIP), 25-28 Sept. 2016, 4448-4452, 10.1109/ICIP.2016.7533201,

3) *Line 92, please add a bit more information about Gaussian smoothing.*

### Authors' response:

Thanks for your suggestion. In response, we have expanded the description in Line 92 to read: “*Gaussian smoothing was applied to the vertical profiles to suppress high-frequency noise and reduce the impact of outliers, ensuring smoother transitions between adjacent layers and enhancing the physical interpretability of the vertical structure.*” This added detail clarifies how the smoothing improves the robustness and readability of our retrievals.

4) *Line103, explain why 1064 nm wavelength was selected.*

### Authors' response:

Thanks for your suggestion. In response, we have expanded the text at Line 103 to read: *“For this study, we selected the 1064 nm lidar range-corrected signal strength (RSCS) to retrieve planetary boundary layer height (PBLH) for three reasons. First, the intensity of Rayleigh scattering is inversely proportional to the fourth power of the wavelength, so at 1064 nm the molecular contribution is reduced by a factor of 16 compared to 532 nm, effectively minimizes the contribution from molecular scattering. Second, our Mie-lidar’s 1064 nm channel is optimally matched to the  $\sim 1\ \mu\text{m}$  modal diameter of ambient fine particles, maximizing sensitivity to changes in particle loading at the boundary layer top. Third, in our previous study we have successfully applied 1064 nm RSCS for PBLH detection (Wang et al., 2021), demonstrating both its accuracy and reliability. To avoid incomplete-overlap artifacts, we then applied the gradient method to the RSCS profile above 150 m.”* This addition clarifies our rationale for choosing 1064 nm and highlights its suitability for PBLH detection.

## Reference

Wang, F., Yang, T., Wang, Z., Chen, X., Wang, H., and Guo, J.: A comprehensive evaluation of planetary boundary layer height retrieval techniques using lidar data under different pollution scenarios, *Atmospheric Research*, 253, 105483, <https://doi.org/10.1016/j.atmosres.2021.105483>, 2021.

5) Line 117, please add the grid resolution of CAMS data.

## Authors’ response:

Thanks for your suggestion. We have updated Line 117 to read: *“The vertical concentration data of  $\text{NO}_2$  and ozone ( $\text{O}_3$ ) are sourced from the Copernicus Atmosphere Monitoring Service (CAMS; grid resolution  $0.75^\circ \times 0.75^\circ$ , temporal resolution 3 h; <https://ads.atmosphere.copernicus.eu>), which were also used to calculate the atmospheric oxidizing capacity (AOC) as  $\text{NO}_2 + \text{O}_3$ .”* This addition clarifies the spatial and temporal resolution of the CAMS data used.

6) Line 140, The "Toxic Pollution" category ( $>250\ \mu\text{g}/\text{m}^3$ ) mentioned in the text seems

to have no data support in Fig. 1. Perhaps either delete it or merge it into other categories.

#### Authors' response:

Thanks for your suggestion. We have added the “Toxic Pollution” category ( $>250 \mu\text{g}/\text{m}^3$ ) and relocated all pollution-level-based vertical profile panels to the Supplementary Materials as Figure R3, thereby ensuring that the main figures remain concise while fully supporting each category mentioned in the text.

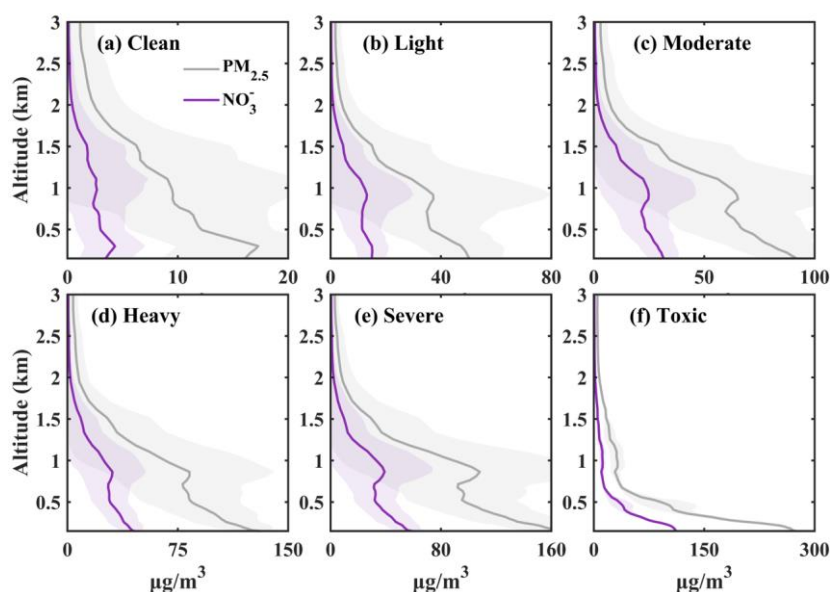


**Figure R3. Vertical profiles of PM<sub>2.5</sub> and nitrate mass concentrations under different pollution conditions.**

7) Line 140-143, Peak height correlates with the boundary layer structure. Does the peak at 900-m reach the top of the inversion layer?

#### Authors' response:

Thanks for your suggestion. The atmospheric boundary-layer top was calculated using the gradient method, so its height closely approximates the inversion layer top. Comparing the 900 m concentration peak height with the mean planetary boundary-layer height (PBLH) under each pollution scenario (Table R1) shows that PBLH exceeds 900 m except during serious pollution, when it falls below that level. Under clean to heavy polluted conditions, 900 m lies within the boundary layer and the

observed concentration maximum results from the inversion inhibiting vertical dispersion. However, during severe pollution, 900 m is above the boundary-layer top (inversion), indicating that the PM<sub>2.5</sub> or nitrate peak arises from the combined effects of secondary in situ formation, vertical transport within the boundary layer, and long-range horizontal advection aloft, producing a localized maximum.

Table R1. Mean PBLH under different pollution conditions

Pollution Level	Clean	Light	Moderate	Heavy	Severe
Mean PBLH (m)	1381.4	1101.1	1058.2	965.7	700.2

8) Figure 5: too much information. Please split and simplify the figure.

#### Authors' response:

Thank you for this suggestion. We have divided the original Figure 5 into two parts: the correlation panel (formerly Figure 5a) has been redrawn as Figure R4 and relocated to the Supplementary Materials, and the conceptual panel has been streamlined as Figure R5 by removing redundant annotations and excessive text to enhance clarity.

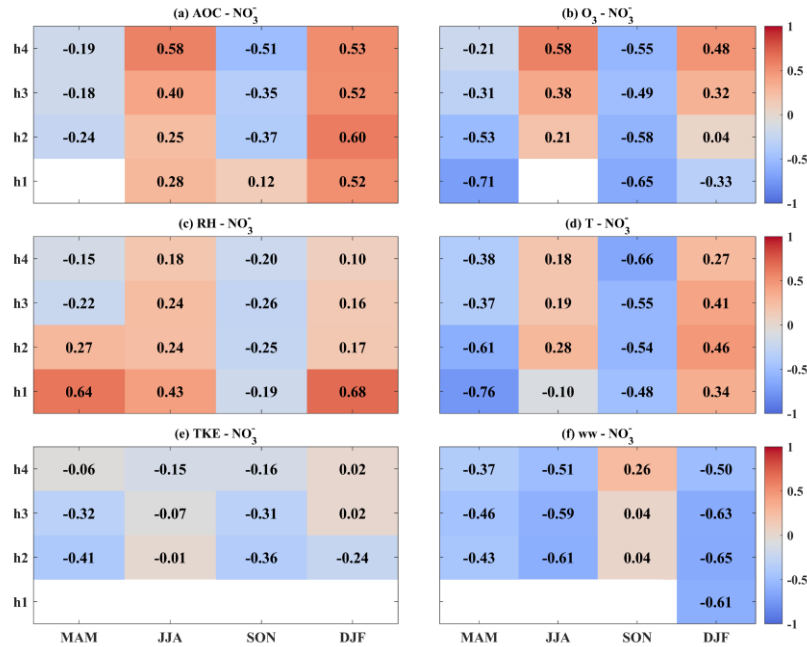


**Figure R4. Heatmap of correlations between nitrate and each driven factor across four seasons and four height layers, with blank cells for non-significant correlations.**

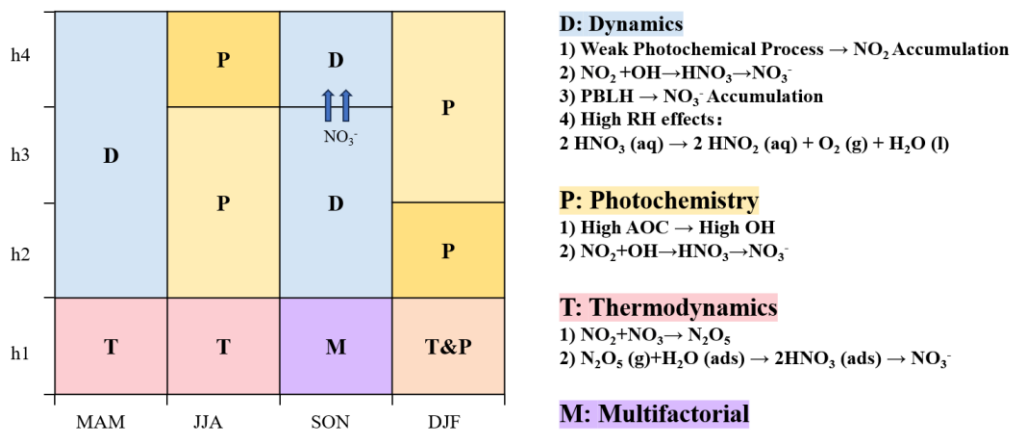


**Figure R5. Vertical distribution of nitrate formation drivers across seasons.**

9) Figure 8: Please add vertical profiles of AOC and NO<sub>2</sub>/O<sub>3</sub> to support the conclusion that "high AOC promotes NO<sub>2</sub> to nitrate, not O<sub>3</sub>".

**Authors' response:**

Thank you for this valuable suggestion. We have added vertical profiles of AOC, NO<sub>2</sub>, and O<sub>3</sub> as a supplementary figure (Figure R6) in the Supplementary Materials. Below 2 km, the AOC and NO<sub>2</sub> profiles closely mirror the nitrate vertical structure shown in Figure 8, whereas the O<sub>3</sub> profile does not, thereby reinforcing our conclusion that high AOC preferentially drives NO<sub>2</sub> conversion to nitrate rather than to O<sub>3</sub>.



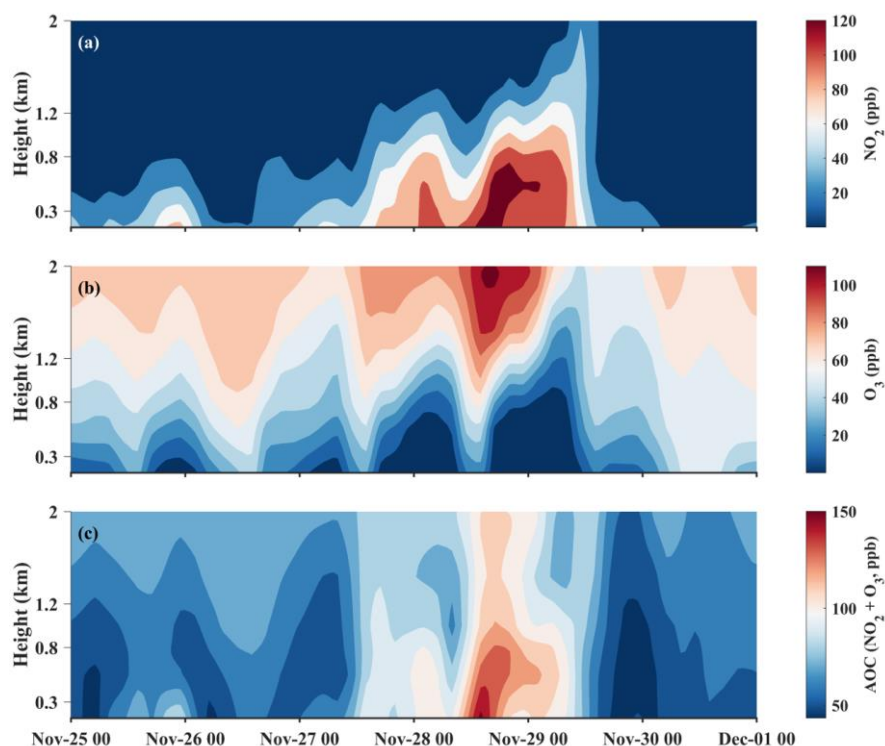


**Figure R6. Vertical profiles of NO<sub>2</sub>, O<sub>3</sub>, and AOC from November 25 to 30, 2021.**

10) Figure 1,4 A bit too many panels. The authors could move the panels f - k to the supplementary materials.

#### **Authors' response:**

Thanks for your suggestion. For Figure 1, we have moved panels f–k as Figure R3 to the Supplementary Materials to enhance clarity. As for Figure 4, we have consolidated the 16 panels into 4 by integrating four height layers for each season into a single panel (Figure R7), which allows for a more concise and clear depiction of the information.

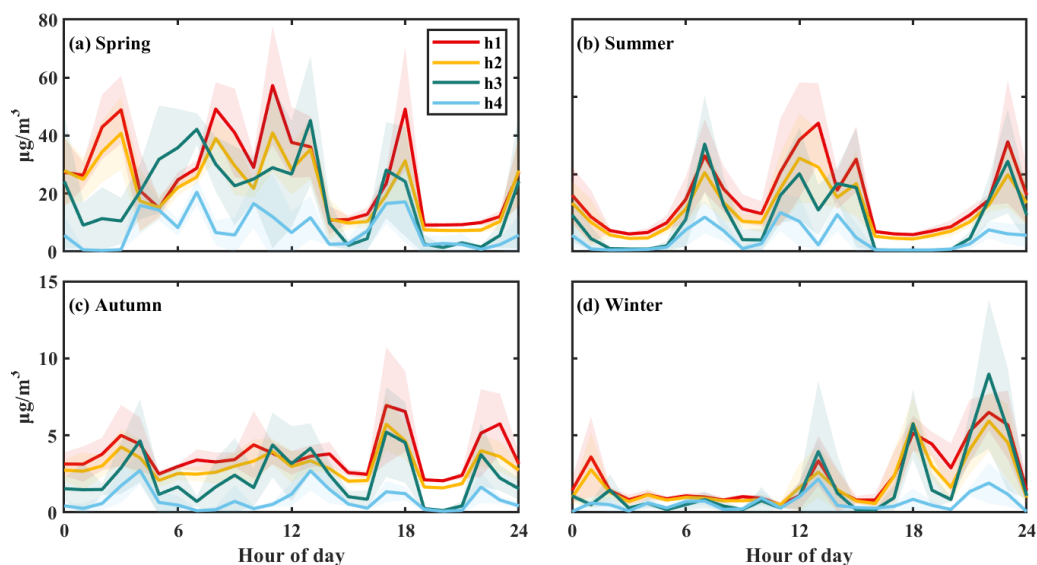


**Figure R7. Diurnal variation of nitrate mass concentrations at four height levels during the four seasons in 2021.**

11) *The number of equations seems odd. Please double check.*

**Authors' response:**

Sorry for the typo. We have corrected it.

12) *Tense check: Please use past tense for the results discussion.*

**Authors' response:**

Thanks for your suggestion. I have adjusted tense of the conclusion in the revised manuscript.

13) *Make sure all citations are listed. For example, Guan et al., 2024 is cited in the introduction but not in the references.*

**Authors' response:**

I'm sorry for the unclear style of reference list. The Guan 2024 have been included in the list. I have changed the style of list to show the reference information clearly.